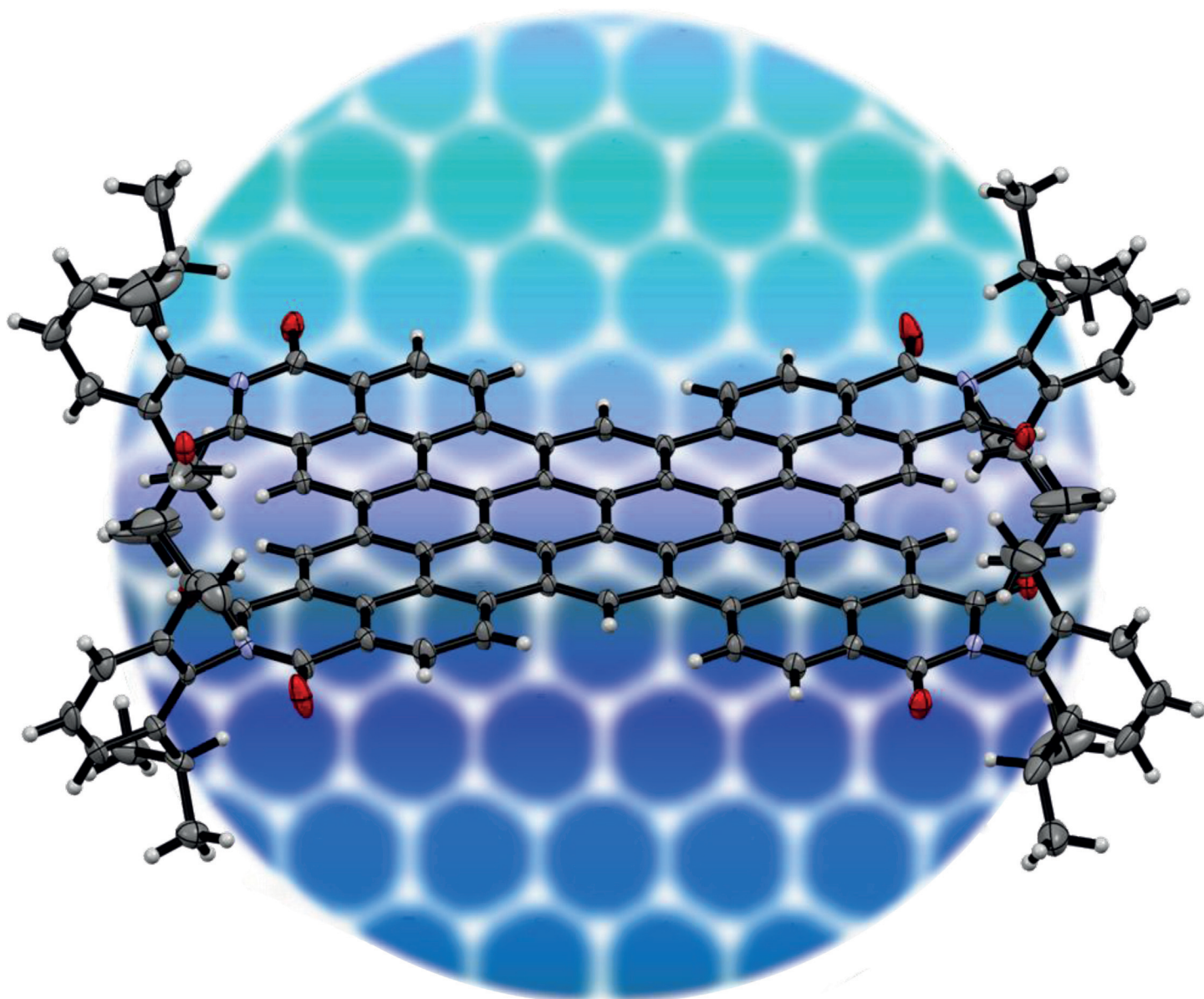


## Polycyclic Aromatics

Deutsche Ausgabe: DOI: 10.1002/ange.201601433  
Internationale Ausgabe: DOI: 10.1002/anie.201601433

# An Electron-Poor C<sub>64</sub> Nanographene by Palladium-Catalyzed Cascade C–C Bond Formation: One-Pot Synthesis and Single-Crystal Structure Analysis

*Sabine Seifert, Kazutaka Shoyama, David Schmidt, and Frank Würthner\***Dedicated to Professor Peter Bäuerle on the occasion of his 60th birthday*

**Abstract:** Herein, we report the one-pot synthesis of an electron-poor nanographene containing dicarboximide groups at the corners. We efficiently combined palladium-catalyzed Suzuki–Miyaura cross-coupling and dehydrohalogenation to synthesize an extended two-dimensional  $\pi$ -scaffold of defined size in a single chemical operation starting from *N*-(2,6-diisopropylphenyl)-4,5-dibromo-1,8-naphthalimide and a tetrasubstituted pyrene boronic acid ester as readily accessible starting materials. The reaction of these precursors under the conditions commonly used for Suzuki–Miyaura cross-coupling afforded a  $C_{64}$  nanographene through the formation of ten C–C bonds in a one-pot process. Single-crystal X-ray analysis unequivocally confirmed the structure of this unique extended aromatic molecule with a planar geometry. The optical and electrochemical properties of this largest ever synthesized planar electron-poor nanographene skeleton were also analyzed.

**P**olycyclic aromatic hydrocarbons (PAHs) are a well-known class of organic molecules that are characterized by extended carbon-rich  $sp^2$ -hybridized scaffolds with interesting electronic properties. Therefore, these types of compounds have attracted considerable interest as promising materials for organic electronics and photovoltaics. Among the broad variety of  $\pi$ -conjugated polycyclic carbon materials, graphenes<sup>[1]</sup> and carbon nanotubes<sup>[2]</sup> have been studied most intensively. Since the first isolation of graphene in 2004,<sup>[3]</sup> numerous graphene nanoribbons as well as nanotube cutouts of different sizes and edge structures have been developed to deduce intrinsic structure–property relationships.<sup>[4]</sup> Likewise, various bowl-shaped corannulenes were investigated in detail as the smallest fragments of fullerene  $C_{60}$ .<sup>[5]</sup> The conventional synthetic strategies for the construction of such PAHs, including heteroatom-containing electron-rich graphene-type molecules, such as annulated porphyrins,<sup>[6]</sup> are based on pioneering work by Scholl<sup>[7]</sup> and Clar,<sup>[8]</sup> and usually include common C–C bond-formation steps, such as Suzuki–Miyaura or Yamamoto cross-couplings, Diels–Alder cycloadditions, or acetylene trimerizations, to prepare the polyaromatic precursors. To ultimately annulate these multiaromatic building blocks for the construction of fully  $\pi$ -conjugated scaffolds, the final carbon–carbon bonds are commonly generated by oxidative dehydrogenation using Lewis acids or oxidants such as  $FeCl_3$ ,  $MoCl_5$ , or DDQ in Scholl-type coupling reactions.<sup>[4a,9]</sup>

Although these multistep procedures are well established for electron-rich PAHs and nanographene derivatives bearing no additional functional groups, synthetic access to larger electron-poor systems as required for n-type semiconductivity remains limited presumably owing to the instability of the carbocation intermediates that are formed from electron-deficient precursors in Scholl-type reactions. Examples accomplished in the past are generally related to electron-poor rylene bisimides, which could be obtained by oxidative dehydrogenation under strongly basic conditions.<sup>[10]</sup> Moreover, the groups of Wang<sup>[11]</sup> and Nuckolls<sup>[12]</sup> reported on extended oligo(rylene bisimides), where the presynthesized monomeric units were connected by Stille or Ullmann couplings followed by Mallory photocyclization or dehydrohalogenation. A somewhat more general synthetic approach towards electron-poor PAHs bearing more than two imide groups is concerned with the preconstruction of PAHs functionalized with anhydrides or carboxylic acid esters and their imidization to generate the corresponding electron-deficient imide analogues.<sup>[13]</sup> In another approach, Feng, Müllen, and co-workers have reported on the atomically precise edge chlorination of nanographene derivatives providing access to electron-deficient halogenated nanographenes.<sup>[14]</sup>

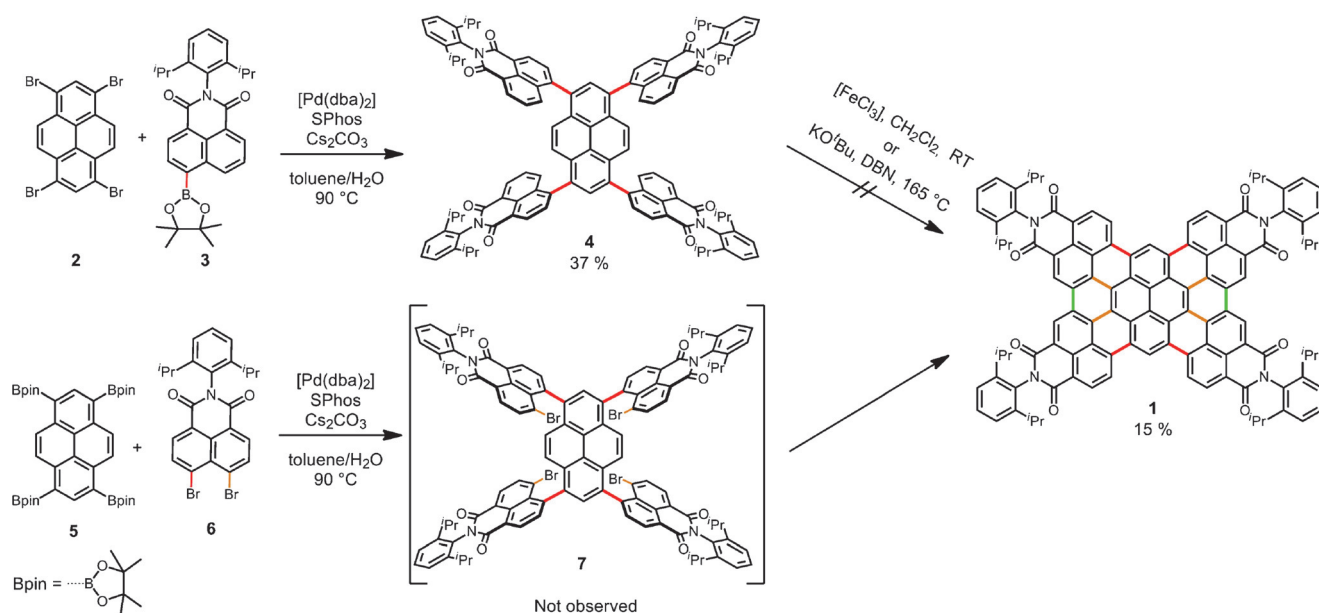
Herein, we describe the direct and highly efficient one-pot synthesis of an electron-poor nanographene bearing four electron-withdrawing naphthalimide groups that are annulated to a pyrene core. Ten carbon–carbon bonds are formed in a single chemical operation by palladium-catalyzed Suzuki–Miyaura cross-coupling, dehydrohalogenation, and oxidative dehydrogenation, leading to the formation and isolation of the electron-poor nanographene **1** with 64  $sp^2$ -hybridized carbon atoms in 15% yield, which is intriguingly high for such systems. Moreover, the molecular structure of this  $\pi$ -extended system was elucidated by single-crystal X-ray analysis, confirming the formation of multiple C–C bonds and the planar geometry of the scaffold.

In our initial attempts to synthesize the electron-poor nanographene **1**, we followed a frequently applied stepwise strategy that includes C–C bond formation by palladium-catalyzed cross-coupling and subsequent oxidative dehydrogenation. Although we could prepare intermediate **4** by Suzuki–Miyaura cross-coupling of 2,6-diisopropylphenyl-substituted naphthalimide boronic acid pinacol ester **3**<sup>[15]</sup> and tetrabrominated pyrene **2**, the subsequent oxidative dehydrogenation under conditions described in the literature<sup>[10a,16]</sup> to generate the annulated system **1** either failed completely or gave only trace amounts of the desired product (Scheme 1, top). Therefore, after reacting pyrene derivative **4** with iron(III) chloride as an oxidant, the starting compound was recovered without any noticeable conversion. Obviously, the oxidation strength of  $FeCl_3$  seems not to be sufficient to dehydrogenate this electron-poor molecule to a  $\pi$ -extended framework. Another explanation might be that the potential for the formation of new carbon–carbon bonds is significantly reduced at the 4-, 5-, 9-, and 10-positions of the pyrene radical cations as suggested by Lorbach et al.<sup>[17]</sup> based on their quantum-chemical calculations of the spin density distribution in such species. Likewise, the dehydrogenation of **4** under

[\*] S. Seifert, Dr. K. Shoyama, Dr. D. Schmidt, Prof. Dr. F. Würthner  
Universität Würzburg, Institut für Organische Chemie and Center for  
Nanosystems Chemistry  
Am Hubland, 97074 Würzburg (Germany)  
E-mail: wuerthner@chemie.uni-wuerzburg.de

Supporting information for this article can be found under:  
<http://dx.doi.org/10.1002/anie.201601433>.

© 2016 The Authors. Published by Wiley-VCH Verlag GmbH & Co. KGaA. This is an open access article under the terms of the Creative Commons Attribution Non-Commercial NoDerivs License, which permits use and distribution in any medium, provided the original work is properly cited, the use is non-commercial, and no modifications or adaptations are made.



**Scheme 1.** Synthetic routes to electron-poor nanographene **1**. dba = dibenzylideneacetone, DBN = 1,5-diazabicyclo[4.3.0]non-5-ene, SPhos = 2-dicyclohexylphosphino-2',6'-dimethoxybiphenyl.

strongly basic conditions, which were previously applied for C–C bond formation,<sup>[10a]</sup> gave only minor amounts of the respective ring-fused product along with some partially cyclized side products, which could not be separated from each other. To increase the driving force for the intramolecular ring-closure reaction, we changed our strategy and introduced an additional halogen atom next to the reaction center for Suzuki–Miyaura cross-coupling, anticipating a subsequent facile dehydrohalogenation reaction similar to literature-known procedures for pyrenes and other polyarenes.<sup>[18]</sup> Accordingly, we repeated our initial Suzuki–Miyaura cross-coupling reaction, but this time using tetraboronated pyrene **5**<sup>[19]</sup> and dibrominated naphthalimide **6**<sup>[20]</sup> as the coupling components (Scheme 1, bottom). To our surprise, under the standard reaction conditions as applied before, we observed the direct formation of the fully conjugated compound **1** by C–C cross-coupling (highlighted in red), intramolecular dehydrohalogenation (highlighted in orange), and, more intriguingly, additional C–C bond formation between adjacent naphthalimide moieties formally by oxidative dehydrogenation (highlighted in green). In total, ten C–C bonds were formed in this one-pot synthesis, affording the electron-poor nanographene **1** in a, for such systems remarkably, high yield of 15% without detectable formation of intermediate **7** (also shown in Scheme 1) or any partially annulated side products.

The new electron-poor nanographene **1** was characterized by <sup>1</sup>H and <sup>13</sup>C NMR spectroscopy, high-resolution mass spectrometry, and elemental analysis. Furthermore, single crystals suitable for X-ray analysis could be grown by slow diffusion of hexane into a solution of **1** in chloroform (for details, see the Supporting Information), and thus its molecular structure could be unambiguously confirmed (Figure 1; see also the Supporting Information, Figure S4). Owing to the four bulky diisopropylphenyl substituents, nanographene **1** displays a large longitudinal and transversal intermolecular

displacement of approximately 14 Å, whereas each individual molecule is intercalated by four symmetry equivalents through C–H...π interactions (Figure 1b). As a consequence of the intercalation of the diisopropylphenyl substituents between the π-surfaces, a large π–π distance of 13.30 Å was observed, giving rise to a brick-wall-type packing arrangement in which the individual layers are separated by chloroform molecules (Figure S4b,c). Furthermore, several solvent-accessible voids exist within these layers (Figure S4b,c), which describe the squeezed electron density of highly disordered chloroform molecules and could not be modeled satisfactorily. In contrast to other graphene cutouts, such as teranthene or quarteranthene,<sup>[21]</sup> in which quinoidal resonance structures with biradicaloid character are established by the propensity of the π-scaffold to increase the number of Clar sextets,<sup>[22]</sup> nanographene **1** does not exhibit a systematic C–C bond-length alternation. Instead, the overall mean bond length of **1** (1.413 Å) is comparable to that of infinite graphene (1.415 Å),<sup>[23]</sup> although the benzenoid C–C bonds (1.409 Å; Figure 1c, shaded in red) are somewhat shorter than the interconnecting carbon–carbon bonds (1.436 Å; Figure 1c, marked in blue). Similar bond-length characteristics have been observed for disc-shaped nanographenes<sup>[14]</sup> and coronenes<sup>[24]</sup> by X-ray analysis. With an almost coplanar π-surface of approximately 118 Å<sup>2</sup> that is generated by 64 fully conjugated carbon and 4 nitrogen atoms, compound **1** is one of the largest planar PAHs whose molecular structure has been determined by X-ray analysis. Somewhat smaller electron-rich flat nanographene derivatives were crystallographically characterized by Kubo and co-workers with sp<sup>2</sup> carbon atom counts of C<sub>42</sub> (teranthene, ca. 71 Å<sup>2</sup>) and C<sub>56</sub> (quarteranthene, ca. 98 Å<sup>2</sup>).<sup>[21]</sup> In contrast, all nanographenes with an even higher carbon content of C<sub>80</sub><sup>[5c]</sup> or C<sub>96</sub><sup>[14]</sup> that have been reported thus far showed strongly distorted π-scaffolds owing to the incorporation of odd-membered



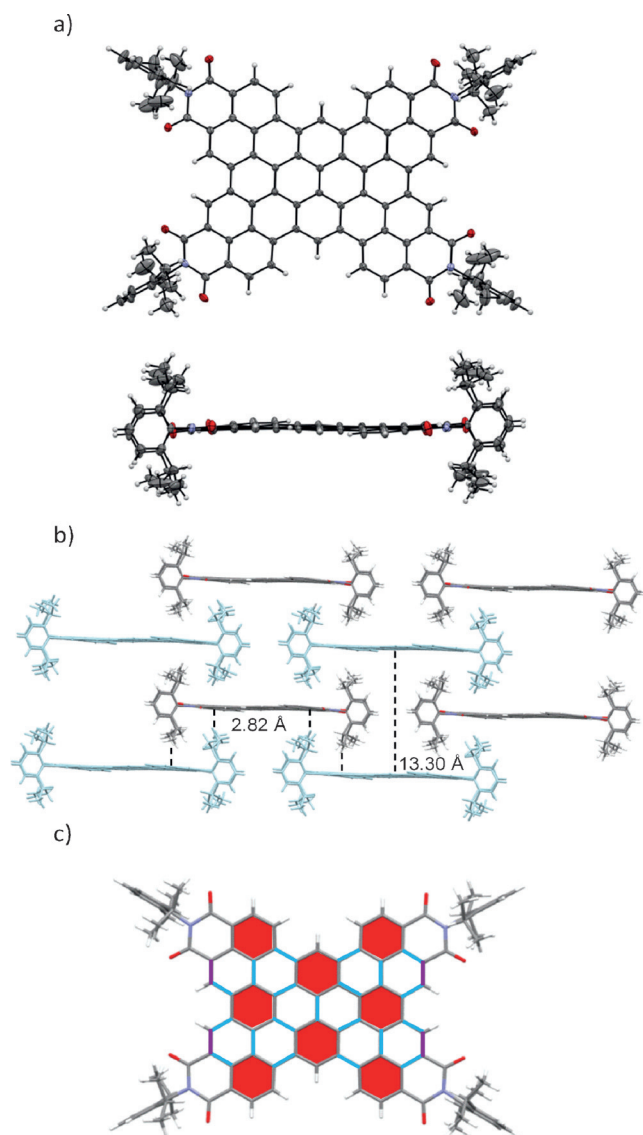


**Figure 1.** a) Solid-state molecular structure of nanographene **1** determined by single-crystal X-ray diffraction (top: front view, bottom: side view; ellipsoids set at 50% probability). b) The packing arrangement of **1** (solvent molecules omitted for clarity). c) Visualization of the different C–C bonds. Bonds within benzenoid rings (shaded in red): 1.382–1.436 Å (avg. 1.409 Å), bonds connecting benzenoid rings (in blue): 1.418–1.466 Å (avg. 1.436 Å), olefinic bonds (in violet): 1.363 Å.

rings or steric constraints at the edges of the disc-shaped molecules.

To experimentally assess the frontier molecular orbitals of **1**, cyclic and square-wave voltammetry (Figure S2, Table S2) was performed. Interestingly, one oxidation and four not fully separated reduction processes were observed, which could only be resolved by square-wave voltammetry (Figure S2). These redox events with potentials of +1.03, –0.99, –1.18, –1.59, and –1.68 V exhibited roughly the same integrated current, indicating single-electron-transfer processes. Considering the energy level of ferrocene/ferrocenium (Fc/Fc<sup>+</sup>) with respect to the vacuum level (–4.8 eV),<sup>[25]</sup> the HOMO and LUMO energy levels of **1** can be estimated using its

experimentally determined redox potentials. The obtained values of –3.81 eV for the LUMO and –5.83 eV for the HOMO level (Figure 2) are in good agreement with our DFT calculations. Comparable LUMO levels were reported for other electron-poor PAHs, such as chlorinated nanographenes (–3.37 to –4.01 eV),<sup>[14]</sup> bay-unsubstituted perylene bisimides (ca. –3.85 eV),<sup>[26]</sup> or fullerene derivatives such as PC<sub>60</sub>BM (–3.91 eV).<sup>[27]</sup> Therefore, the electron-poor C<sub>64</sub> nanographene **1** constitutes a novel prototype for two-dimensional organic electron-acceptor materials that should be of interest for (opto)electronic devices.

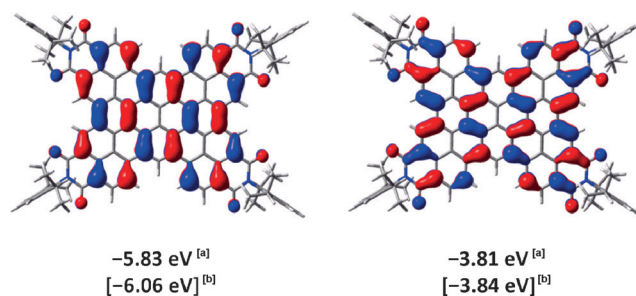


**Figure 2.** HOMO (left) and LUMO (right) of compound **1** calculated by DFT (B3-LYP, def2-SVP, isoval: 0.02 a.u.). [a] Calculated according to literature-known procedures using the experimentally determined redox potentials ( $E_{\text{LUMO}} = -[E(\text{M}/\text{M}^-) + 4.8 \text{ eV}]$  and  $E_{\text{HOMO}} = -[E(\text{M}/\text{M}^+) + 4.8 \text{ eV}]$ ) and the energy level of ferrocene/ferrocenium (Fc/Fc<sup>+</sup>) with respect to the vacuum level (–4.8 eV).<sup>[25]</sup> [b] DFT calculated values (B3-LYP, def2-SVP).

The optical properties of the annulated scaffold **1** were characterized by UV/Vis absorption and fluorescence spectroscopy in dichloromethane at room temperature (Figures 3 and S1, Table S1). The  $\pi$ -extended PAH **1** displayed distinct absorption spectral features with remarkably high molar absorptivities in the visible range (Figure 3). Similar to other two-dimensional PAH scaffolds, such as pyrenes,<sup>[28]</sup> coronenes,<sup>[13a]</sup> or hexabenzocoronenes,<sup>[29]</sup> the absorption spectrum of **1** is not dominated anymore by the lowest-energy S<sub>0</sub>–S<sub>1</sub> transition ( $\lambda_{\text{max}} = 584 \text{ nm}$ ,  $\epsilon_{\text{max}} = 141\,200 \text{ M}^{-1} \text{ cm}^{-1}$ ) but by a higher-energy absorption band at  $\lambda_{\text{max}} = 489 \text{ nm}$ , which is characterized by well-resolved vibronic progressions and

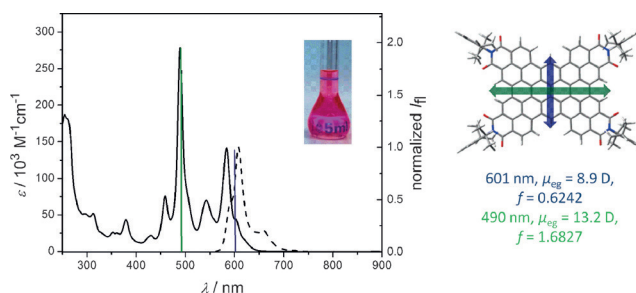


**Figure 3.** Left: UV/Vis absorption (solid line) and emission spectra (dotted line,  $\lambda_{\text{ex}} = 530 \text{ nm}$ ) of **1** in CH<sub>2</sub>Cl<sub>2</sub> ( $c \approx 1 \times 10^{-5} \text{ M}$ ) at room temperature. Inset: Photograph of a CH<sub>2</sub>Cl<sub>2</sub> solution of **1**. Right: Calculated transitions (blue and green lines), transition dipole moments ( $\mu_{\text{eg}}$ ), and oscillator strengths ( $f$ ) of **1** determined by TD-DFT (B3-LYP, def2-SVP).

a very high molar extinction coefficient of  $278\,300\text{ M}^{-1}\text{ cm}^{-1}$ . According to TD-DFT calculations, the transition dipole moments of these two main transitions are aligned along the short and long molecular axes of the central pyrene core (Figure 3, right). Most interestingly, despite the lower oscillator strength of the lowest-energy transition, bright fluorescence with an absolute quantum yield of  $67 \pm 1\%$  occurs from the first excited singlet state at  $\lambda_{\text{max}} = 608\text{ nm}$  with a mirror-image-like vibronic fine structure. This high fluorescence quantum yield for the 2D fluorophore **1** can be explained by the unusually prolonged fluorescence lifetime of 13.4 ns, which is significantly longer than that of conventional fluorescent dyes, such as perylene bisimides (ca. 4–6 ns).<sup>[30]</sup> The high fluorescence quantum yield and lifetime accordingly appear as promising properties of 2D core-expanded electron-poor polycyclic hydrocarbons that warrant further exploration.

In summary, we have reported an efficient synthetic route towards electron-poor nanographenes by combining palladium-catalyzed Suzuki–Miyaura cross-couplings, dehydrohalogenation, and oxidative dehydrogenation in a cascade reaction. Ten carbon–carbon bonds were thus created in a single chemical operation to yield a planar  $\text{C}_{64}$  nanographene with a size of  $118\text{ Å}^2$ . This nanographene constitutes a first example for a new class of compounds, that is, electron-poor counterparts of hitherto extensively investigated electron-rich PAHs and nanographenes. This archetypical electron-poor 2D  $\pi$ -scaffold could be obtained on preparative scale as required for its full characterization by comprehensive electrochemical and optical studies as well as single-crystal structure analysis. We are convinced that the synthetic procedure reported herein constitutes a general entry into a new class of electron-poor nanosized functional molecules. Accordingly, current efforts in our laboratory are directed towards extending this synthetic method to even larger as well as bowl-shaped nanographene derivatives for applications as high-performance (opto)electronic materials.

## Acknowledgements

We thank the DFG for financial support provided to the research training school GRK 2112 on “Molecular Biradicals”, and Professor Eiichi Nakamura and the University of Tokyo for supporting a four months research stay of K.S. at the Universität Würzburg through the MERIT program.

**Keywords:** cascade reactions · dyes/pigments · nanographene · polycyclic aromatic hydrocarbons · two-dimensional nanostructures

**How to cite:** *Angew. Chem. Int. Ed.* **2016**, *55*, 6390–6395  
*Angew. Chem.* **2016**, *128*, 6500–6505

- [1] a) M. J. Allen, V. C. Tung, R. B. Kaner, *Chem. Rev.* **2010**, *110*, 132–145; b) S. Yang, R. E. Bachman, X. Feng, K. Müllen, *Acc. Chem. Res.* **2013**, *46*, 116–128; c) A. Hirsch, J. M. Englert, F. Hauke, *Acc. Chem. Res.* **2013**, *46*, 87–96.
- [2] A. Hirsch, *Angew. Chem. Int. Ed.* **2002**, *41*, 1853–1859; *Angew. Chem.* **2002**, *114*, 1933–1939.
- [3] K. S. Novoselov, A. K. Geim, S. V. Morozov, D. Jiang, Y. Zhang, S. V. Dubonos, I. V. Grigorieva, A. A. Firsov, *Science* **2004**, *306*, 666–669.
- [4] a) A. Narita, X.-Y. Wang, X. Feng, K. Müllen, *Chem. Soc. Rev.* **2015**, *44*, 6616–6643; b) J. Liu, B.-W. Li, Y.-Z. Tan, A. Giannakopoulos, C. Sanchez-Sanchez, D. Beljonne, P. Ruffieux, R. Fasel, X. Feng, K. Müllen, *J. Am. Chem. Soc.* **2015**, *137*, 6097–6103; c) M. Quernheim, F. E. Golling, W. Zhang, M. Wagner, H.-J. Räder, T. Nishiuchi, K. Müllen, *Angew. Chem. Int. Ed.* **2015**, *54*, 10341–10346; *Angew. Chem.* **2015**, *127*, 10482–10487.
- [5] a) E. A. Jackson, B. D. Steinberg, M. Bancu, A. Wakamiya, L. T. Scott, *J. Am. Chem. Soc.* **2007**, *129*, 484–485; b) M. N. Eliseeva, L. T. Scott, *J. Am. Chem. Soc.* **2012**, *134*, 15169–15172; c) K. Kawasumi, Q. Zhang, Y. Segawa, L. T. Scott, K. Itami, *Nat. Chem.* **2013**, *5*, 739–744; d) S. Da Ros, A. Linden, K. K. Baldrige, J. S. Siegel, *Org. Chem. Front.* **2015**, *2*, 626–633; e) A. K. Dutta, A. Linden, L. Zoppi, K. K. Baldrige, J. S. Siegel, *Angew. Chem. Int. Ed.* **2015**, *54*, 10792–10796; *Angew. Chem.* **2015**, *127*, 10942–10946.
- [6] a) A. Tsuda, A. Osuka, *Science* **2001**, *293*, 79–82; b) T. Tanaka, A. Osuka, *Chem. Soc. Rev.* **2015**, *44*, 943–969.
- [7] R. Scholl, J. Mansfeld, *Ber. Dtsch. Chem. Ges.* **1910**, *43*, 1734–1746.
- [8] E. Clar, *Chem. Ber.* **1948**, *81*, 52–63.
- [9] M. Grzybowski, K. Skonieczny, H. Butenschön, D. T. Gryko, *Angew. Chem. Int. Ed.* **2013**, *52*, 9900–9930; *Angew. Chem.* **2013**, *125*, 10084–10115.
- [10] a) T. Sakamoto, C. Pac, *J. Org. Chem.* **2001**, *66*, 94–98; b) F. Nolde, J. Qu, C. Kohl, N. G. Pschirer, E. Reuther, K. Müllen, *Chem. Eur. J.* **2005**, *11*, 3959–3967.
- [11] a) H. Qian, F. Negri, C. Wang, Z. Wang, *J. Am. Chem. Soc.* **2008**, *130*, 17970–17976; b) W. Yue, A. Lv, J. Gao, W. Jiang, L. Hao, C. Li, Y. Li, L. E. Polander, S. Barlow, W. Hu, S. Di Motta, F. Negri, S. R. Marder, Z. Wang, *J. Am. Chem. Soc.* **2012**, *134*, 5770–5773.
- [12] a) Y. Zhong, B. Kumar, S. Oh, M. T. Trinh, Y. Wu, K. Elbert, P. Li, X. Zhu, S. Xiao, F. Ng, M. L. Steigerwald, C. Nuckolls, *J. Am. Chem. Soc.* **2014**, *136*, 8122–8130; b) Y. Zhong, M. T. Trinh, R. Chen, G. E. Purdum, P. P. Khlyabich, M. Sezen, S. Oh, H. Zhu, B. Fowler, B. Zhang, W. Wang, C.-Y. Nam, M. Y. Sfeir, C. T. Black, M. L. Steigerwald, Y.-L. Loo, F. Ng, X. Y. Zhu, C. Nuckolls, *Nat. Commun.* **2015**, *6*, 8242.
- [13] a) S. Alibert-Fouet, I. Seguy, J.-F. Bobo, P. Destruel, H. Bock, *Chem. Eur. J.* **2007**, *13*, 1746–1753; b) T. V. Pho, F. M. Toma, M. L. Chabiny, F. Wudl, *Angew. Chem. Int. Ed.* **2013**, *52*, 1446–1451; *Angew. Chem.* **2013**, *125*, 1486–1491.
- [14] Y.-Z. Tan, B. Yang, K. Parvez, A. Narita, S. Osella, D. Beljonne, X. Feng, K. Müllen, *Nat. Commun.* **2013**, *4*, 2646.
- [15] W. Sun, W. Li, J. Li, J. Zhang, L. Du, M. Li, *Tetrahedron* **2012**, *68*, 5363–5367.
- [16] Y. Avlasevich, K. Müllen, *J. Org. Chem.* **2007**, *72*, 10243–10246.
- [17] D. Lorbach, M. Wagner, M. Baumgarten, K. Müllen, *Chem. Commun.* **2013**, *49*, 10578–10580.
- [18] a) H. A. Wegner, H. Reisch, K. Rauch, A. Demeter, K. A. Zachariasse, A. de Meijere, L. T. Scott, *J. Org. Chem.* **2006**, *71*, 9080–9087; b) T. Jin, J. Zhao, N. Asao, Y. Yamamoto, *Chem. Eur. J.* **2014**, *20*, 3554–3576.
- [19] R. S. Sprick, J.-X. Jiang, B. Bonillo, S. Ren, T. Ratvijitvech, P. Guiglion, M. A. Zwijnenburg, D. J. Adams, A. I. Cooper, *J. Am. Chem. Soc.* **2015**, *137*, 3265–3270.
- [20] Z. Sun, K.-W. Huang, J. Wu, *Org. Lett.* **2010**, *12*, 4690–4693.
- [21] a) A. Konishi, Y. Hirao, M. Nakano, A. Shimizu, E. Botek, B. Champagne, D. Shiomi, K. Sato, T. Takui, K. Matsumoto, H. Kurata, T. Kubo, *J. Am. Chem. Soc.* **2010**, *132*, 11021–11023; b) A. Konishi, Y. Hirao, K. Matsumoto, H. Kurata, R. Kishi, Y. Shigeta, M. Nakano, K. Tokunaga, K. Kamada, T. Kubo, *J. Am. Chem. Soc.* **2013**, *135*, 1430–1437.
- [22] E. Clar, *The Aromatic Sextet*, Wiley, London, **1972**.

- [23] M. Weinert, E. Wimmer, A. J. Freeman, *Phys. Rev. B* **1982**, 26, 4571–4578.
- [24] Q. Zhang, H. Peng, G. Zhang, Q. Lu, J. Chang, Y. Dong, X. Shi, J. Wei, *J. Am. Chem. Soc.* **2014**, 136, 5057–5064.
- [25] I. Seguy, P. Jolinet, P. Destruel, R. Mamy, H. Allouchi, C. Courseille, M. Cotrait, H. Bock, *ChemPhysChem* **2001**, 2, 448–452.
- [26] R. Schmidt, J. H. Oh, Y. S. Sun, M. Deppisch, A. M. Krause, K. Radacki, H. Braunschweig, M. Könemann, P. Erk, Z. A. Bao, F. Würthner, *J. Am. Chem. Soc.* **2009**, 131, 6215–6228.
- [27] Y. He, Y. Li, *Phys. Chem. Chem. Phys.* **2011**, 13, 1970–1983.
- [28] A. G. Crawford, A. D. Dwyer, Z. Liu, A. Steffen, A. Beeby, L.-O. Pålsson, D. J. Tozer, T. B. Marder, *J. Am. Chem. Soc.* **2011**, 133, 13349–13362.
- [29] Z. Wang, Ž. Tomović, M. Kastler, R. Pretsch, F. Negri, V. Enkelmann, K. Müllen, *J. Am. Chem. Soc.* **2004**, 126, 7794–7795.
- [30] F. Würthner, *Chem. Commun.* **2004**, 1564–1579.

Received: February 9, 2016

Published online: April 5, 2016